GEOPHYSICAL RESEARCH LETTERS, VOL. 36, L05601, doi:10.1029/2008GL036792, 2009

Vertical mixing at intermediate depths in the Arctic boundary current

Y. D. Lenn,[1] P. J. Wiles,[1] S. Torres-Valdes,[2] E. P. Abrahamsen,[3] T. P. Rippeth,[1] J. H. Simpson,[1] S. Bacon,[2] S. W. Laxon,[4] I. Polyakov,[5] V. Ivanov,[5] and S. Kirillov[6]

Received 25 November 2008; revised 5 January 2009; accepted 22 January 2009; published 3 March 2009.

[1] Microstructure and hydrographic observations, during September 2007 in the boundary current on the East Siberian continental slope, document upper ocean stratification and along-stream water mass changes. A thin warm surface layer overrides a shallow halocline characterized by a ~40-m thick temperature minimum layer beginning at ~30 m depth. Below the halocline, well-defined thermohaline diffusive staircases extended downwards to warm Atlantic Water intrusions found at 200–800 m depth. Observed turbulent eddy kinetic energy dissipations are extremely low ($\epsilon < 10^{-6}$ W m^{-3}), such that double diffusive convection dominates the vertical mixing in the upper-ocean. The diffusive convection heat fluxes F_H^{dc} ~1 W m^{-2}, are an order of magnitude too small to account for the observed along-stream cooling of the boundary current. Our results implicate circulation patterns and the influence of shelf waters in the evolution of the boundary current waters. **Citation:** Lenn, Y. D., et al. (2009), Vertical mixing at intermediate depths in the Arctic boundary current, *Geophys. Res. Lett.*, *36*, L05601, doi:10.1029/2008GL036792.

1. Introduction

[2] Record-breaking minimum sea-ice levels observed in summer 2007 [*Perovich et al.*, 2008], highlight the rapid response of the Arctic to climate change. In the Arctic Ocean, the sea-ice floats on cold fresh polar mixed layer that is separated by a shallow halocline from the warm dense North Atlantic Water (AW) circulating counter-clockwise from Fram Strait [e.g., *Meincke et al.*, 1997]. Various imperfectly-understood mechanisms involving Pacific waters from Bering Strait, light and dense continental shelf waters, melting sea-ice and the warm AW are thought to contribute to halocline-formation and upper ocean stratification [*Carmack*, 2000]. A comprehensive understanding of the processes setting upper-ocean stratification is clearly crucial for improving predictions of future Arctic Ocean circulation.

[3] The Arctic boundary current flows along the continental slope, exposing an intermediate-depth (below the halocline and above 1000-m) warm salty AW core to influence of the Arctic marginal shelf seas [*Rudels et al.*, 1999]. Evidence of diffusive convection and salt fingering above and below intrusive layers in the AW core [*Rudels et al.*, 1999] implicate double diffusive processes in transferring heat and salt through the Arctic thermocline. Turbulent dissipation is weak in the Arctic interior [*Rainville and Winsor*, 2008], but may still be important for diapycnal mixing along the boundaries and in marginal seas [*Sundfjord et al.*, 2007]. However, the lack of concurrent measurements of turbulent dissipation, and temperature (T) and salinity (S) fine-structure has precluded a direct comparison of turbulent mixing and double-diffusive processes in the Arctic boundary current. New hydrography and microstructure shear, T and conductivity (C) observations made during the Arctic Synoptic Basin-wide Oceanography (ASBO) ice-free 2007 summer field season, provide an unprecedented opportunity to evaluate the role of vertical mixing in the Arctic Ocean boundary current evolution in the vicinity of the Lomonosov Ridge (hereafter LR, see Figure 1).

2. Data and Methods

[4] The ASBO observations were taken during a joint cruise with the Nansen and Amundsen Basins Observational System (NABOS) research program aboard the Russian research vessel *Viktor Buynitsky*. In this region, the intermediate-depth warm AW core of the boundary current is typically located over bathymetry 500–3000 m deep [*Environmental Working Group*, 1997–1998]. The boundary current bifurcates at LR into the Amundsen Basin (AB) recirculating current and a boundary current remnant that crosses LR to enter the Makarov Basin (MB) where it converges with the MB recirculating current (Figure 1) [*Rudels et al.*, 1994]. This study focuses on three cross-slope upper-ocean sections (Figure 1): Western (W: stations 4–10), Ridge (R: stations 16–23) and Eastern (E: stations 34–40) observed during 18–25 September 2007. Microstructure measurements to 600 m depth were made with a Rockland Scientific International VMP-500 fitted with microstructure shear, T and C probes and an accelerometer. Independent T and C data were obtained from concurrent upper-ocean hydrographic casts, typically to depths not greater than 1200 m, using a Sea-Bird Electronics 19+ CTD and calibrated to bottle salinities. Seawater samples for the determination of nutrients, barium isotopes and δ^{18}O concentrations were also collected and are discussed in a separate study on freshwater composition (E. P. Abrahamsen et al., Tracer-derived freshwater composition of the Siberian Continental Shelf following the extreme Arctic summer of 2007, submitted to *Geophysical Research Letters*, 2009).

[5] Microstructure shear, T and C profiles from the VMP, in free-fall mode with typical fall speeds of ~0.65 m s^{-1}, were obtained at each station (Figure 1) with repeat profiles as time allowed. The shear data were edited to exclude near-

[1]School of Ocean Sciences, Bangor University, Bangor, UK.
[2]National Oceanography Centre, Southampton, UK.
[3]British Antarctic Survey, Natural Environment Research Council, Cambridge, UK.
[4]Centre for Polar Observation and Modelling, University College London, London, UK.
[5]International Arctic Research Center, University of Alaska Fairbanks, Fairbanks, Alaska, USA.
[6]Arctic and Antarctic Research Institute, St. Petersburg, Russia.

0094-8276/09/2008GL036792$05.00

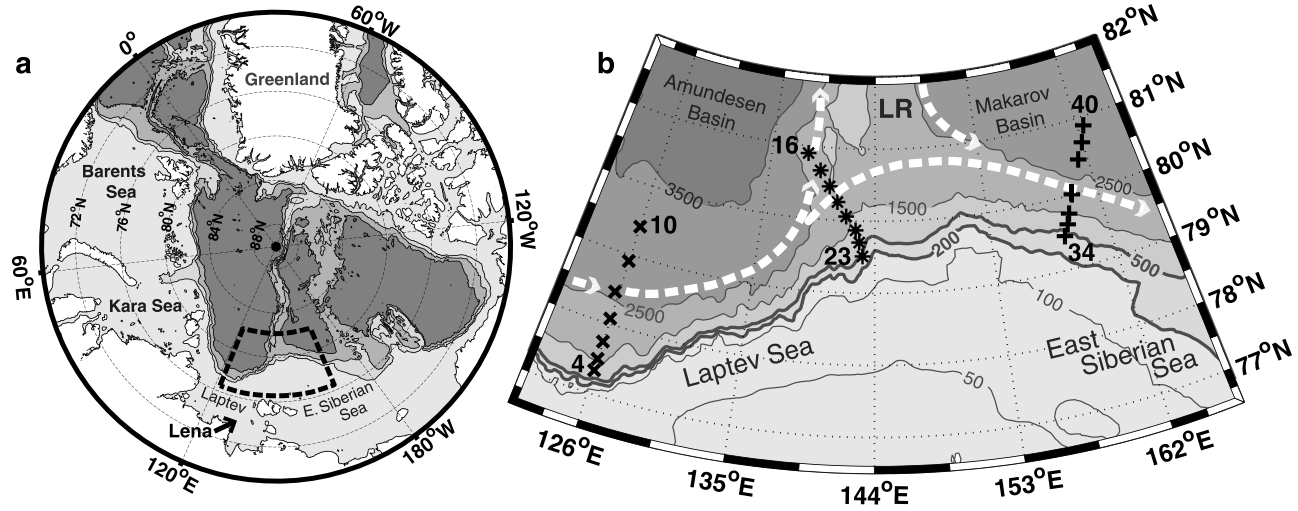

Figure 1. (a) Arctic Ocean bathymetry with land shaded gray and the ASBO 2007 study region outline by the thick dashed line. (b) Location of the 2007 ASBO boundary current observations: Western (crosses), Ridge (asterisks) and Eastern (pluses) slope sections. Bathymetry is contoured in grayscale; thicker contours pick out the 200-m and 500-m isobaths. Dashed white arrows indicate the boundary/recirculating currents suggested by *Rudels et al.* [1994]. Locations of the Barents, Kara, Laptev and East Siberian Seas, Amundsen Basin, Lomonosov Ridge (LR) and Makarov Basin are marked.

surface observations susceptible to ship-wake turbulence, post-bottom impact data, and anomalous data spikes. Microstructure T and C data, with ~1 cm vertical resolution, were calibrated to on-station CTD measurements. Following *Rippeth et al.* [2003], turbulent kinetic energy (tke) dissipation was estimated as $\epsilon = 7.5\mu\langle u_z^2\rangle$ W m^{-3}, where $\mu = 1.88 \times 10^{-3}$ J m^{-3} s is the dynamic viscosity of seawater and angle brackets denote vertical averaging of the shear-squared (u_z^2) over 2-second intervals (~1.3 m depth). Where section/depth-averaged values of ϵ or other quantities are presented, standard errors are given throughout.

3. Boundary Current Waters

[6] On all three cross-sections, warm fresh surface waters lie above a ~40-m thick T minimum layer occurring in the 30–70 m depth range (Figures 2a and 2b). The relatively warm near-surface T (>−1°C at 10 m depth, Figure 2a) are most likely due to direct insolation [*Perovich et al.*, 2008]. Minimum upper-ocean T are clustered at −1.8°C on sections W and R (Figure 2a), and are slightly warmer on section E. Above 70 m, the boundary current waters freshen downstream, with the deepest halocline found on the freshest section E (Figure 2b). Phosphate and δ^{18}O data collected during the cruise indicate that the deepening of the halocline is mostly due to high amounts of river discharge with a contribution from Pacific-source water (Abrahamsen et al., submitted manuscript, 2009). It is clear from the buoyancy frequency (N^2) profiles (Figure 2c) that the stratification here is dominated by salinity, as N^2 is generally very low (<10^{-4} s^{-2}) except at halocline depths.

[7] As at other Arctic locations [e.g., *Rudels et al.*, 1999], the sub-surface AW-core T maximum is characterized by intrusive layers that are distinguished by sharp inversions easily traced between adjacent stations and along-stream in the potential temperature-S (θ-S) diagrams (Figure 2d). These intrusions are thought to form at the confluence of two AW branches [e.g., *May and Kelley*, 2001]: a warmer saltier off-shore branch flowing as a continental-slope boundary current from Fram Strait, and a cooler fresher inshore branch that has undergone winter sea-air heat loss and dilution by shelf water in the Barents Sea before rejoining the boundary current near the St. Anna Trough (north Kara Sea) [e.g., *Schauer et al.*, 2002]. The intermediate-depth AW core is a source of heat and salt for the polar mixed layer and the deep Arctic Ocean.

[8] This study focuses on the dramatic changes occurring along-stream above 250 m depth where the current cools (Figure 2a) and freshens (Figure 2b inset) markedly eastwards; the biggest cooling occurs between sections W and R. The boundary current changes are best quantified by differences in upper ocean heat content, $\Delta HC = \rho c_p \int Tdz$, where $c_p = 3900$ J kg^{-1} K^{-1} is the specific heat of seawater. We calculated the mean heat content differences between adjacent cross-sections ($\Delta HC_{WR/RE}$) for the upper 250 m, beginning at 100-m depth so as to exclude consideration of surface heat fluxes: ΔHC_{WR} is $-4.8 \pm 0.5 \times 10^8$ J m^{-2} and ΔHC_{RE} is $-1.9 \pm 0.5 \times 10^8$ J m^{-2}. Assuming that the slope sections provide a synoptic view of the boundary current, then the observed heat loss can only be explained by either vertical exchange due to turbulent or doubly-diffusive heat fluxes, or lateral exchange with the Arctic interior basins or continental shelves. Quantifying the heat loss through vertical mixing from AW-core towards the air/ice-ocean interface is of particular relevance to Arctic climate change.

4. Vertical Exchange

[9] Diffusive staircases have been observed elsewhere in the Arctic [e.g., *Rudels et al.*, 1999], but rarely with the resolution of the ASBO-2007 microstructure data. Well-defined thermohaline staircases consisting of well-mixed layers (~5 cm to ~60 m thick) separated by sharp interfaces are present in the Siberian continental slope microstructure

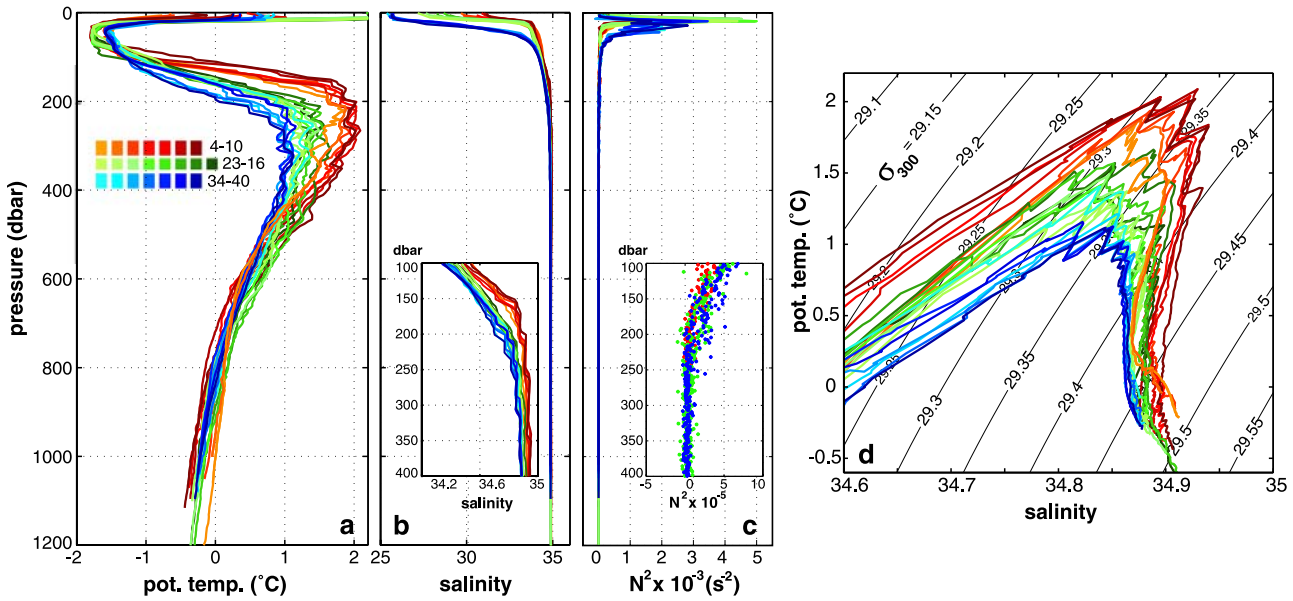

Figure 2. Upper ocean CTD observations of (a) potential temperature (θ°C), (b) salinity and (c) Brunt-Väisälä buoyancy frequency (N^2 s^{-2}) along the three cross-slope sections. Insets show CTD salinities (Figure 2b) and section-mean high-resolution N^2 profiles inferred from 2-second averaged microstructure T/S (Figure 2c). (d) The θ-S curves of intrusions in the AW core are plotted with σ_{300} potential density contours. Colour delineates observations from sections W (red), R (green) and E (blue); darker colours indicate increasing distance off-shore.

observations (Figure 3a). Except for infrequent inversions, T and S increase monotonically with depth in the staircases that are better defined on sections W (110–180 m) and E (130–220 m), than on section R (130–220 m); a typical profile from each of the three sections is shown in Figure 3a.

[10] Thermohaline staircases typically occur in weakly turbulent environments or where the turbulence is balanced by layer-advection. Here, the observed ϵ that can be resolved above the instrument noise level ($\sim 2 \times 10^{-7}$ W m^{-3}) is very low at all depths observed below the halocline (Figure 3b): section- and depth-averaged staircase values are $\overline{\epsilon_W} = 5.7 \pm 0.9 \times 10^{-7}$ W m^{-3}, $\overline{\epsilon_R} = 4.6 \pm 1.0 \times 10^{-7}$ W m^{-3}, and $\overline{\epsilon_E} = 8.7 \pm 1.1 \times 10^{-7}$ W m^{-3}. Following *Inoue et al.* [2007] who investigated how buoyancy fluxes are best estimated in mixed turbulent and double diffusive environments, we evaluated the Reynolds number, $Re = \epsilon \mu^{-1} N^{-2}$ as defined by *Gargett* [1988]. According to *Gargett* [1988], the turbulent buoyancy flux, and hence the turbulent mixing of heat and salt, is suppressed by the stratification when $Re < 20$. Estimating N^2 from 2-second running-averaged microstructure T and S profiles ($N^2 \sim 5 \times 10^{-5}$ s^{-2}, Figure 2c inset) gives $Re < 10$ in the thermohaline staircases, implying that the turbulence is insufficiently energetic to drive vertical mixing in the Arctic boundary current.

[11] The stability of the water column to double diffusion, where heat and salt diffuse down-gradient, may be determined from Turner angles [*Ruddick*, 1983], $\mathrm{Tu} = \tan^{-1}[(1 + R_\rho)(1 - R_\rho)^{-1}]$ which depend on the density ratio $R_\rho = \frac{\beta \Delta S}{\alpha \Delta T}$, where α (β) are the coefficients of thermal(haline) expansion, and ΔT and ΔS are the T and S-differences across each step interface. The Tu angles in the thermohaline staircases fall largely within the diffusive convection regime (i.e. $-90° < \mathrm{Tu} < -45°$) and occasionally into the salt-fingering regime (i.e., $45° < \mathrm{Tu} < 90°$) where T-inversions are present (Figures 3a and 3c). Vertical (upwards) heat fluxes through the diffusively-convecting step interfaces are estimated following *Kelley* [1990]: $F_H^{dc} = 0.0032 \rho c_p \exp(4.8 R_\rho^{-0.72})\ (\alpha g \kappa_T^2 / \nu)^{1/3} (\Delta T)^{4/3}$, where ν is kinematic viscosity, κ_T is the molecular diffusivity for heat, and g is the acceleration due to gravity. We found that there was no discernable depth-dependence of F_H^{dc} in the upper-ocean staircase (e.g., Figure 3d). Section and staircase-averaged F_H^{dc} values are: 1.6 ± 0.6 W m^{-2} on section W, 0.91 ± 0.3 W m^{-2} on section R and 0.81 ± 0.2 W m^{-2} on section E (Figure 3d).

[12] Long-term moored NABOS observations of currents on the continental slope north of the Laptev Sea (LS) indicate that mean boundary current velocities in this area are ~2 cm s^{-1} and directed along isobaths [*Dmitrenko et al.*, 2008]. If we assume a maximum vertical heat flux of ~1.6 W m^{-2} through the thermohaline staircase integrated over ~414-km path along the 1500 m isobath between the section W and R, the total heat loss is $\sim 3.36 \times 10^7$ J m^{-2}. Assuming similar current velocities and a maximum vertical heat flux of ~1 W m^{-2}, the heat loss through the thermohaline staircase along the ~393-km path between sections R and E is $\sim 2.0 \times 10^7$ J m^{-2}. These vertical heat fluxes are about an order of magnitude too small to account for the observed heat content changes (Sect. 3).

5. Discussion

[13] The advection of heat and freshwater anomalies resulting from interannual variability in the boundary current source waters can result in boundary current alongstream variability [*Woodgate et al.*, 2001]. The 2003–2005 NABOS observations resolved a large warm anomaly

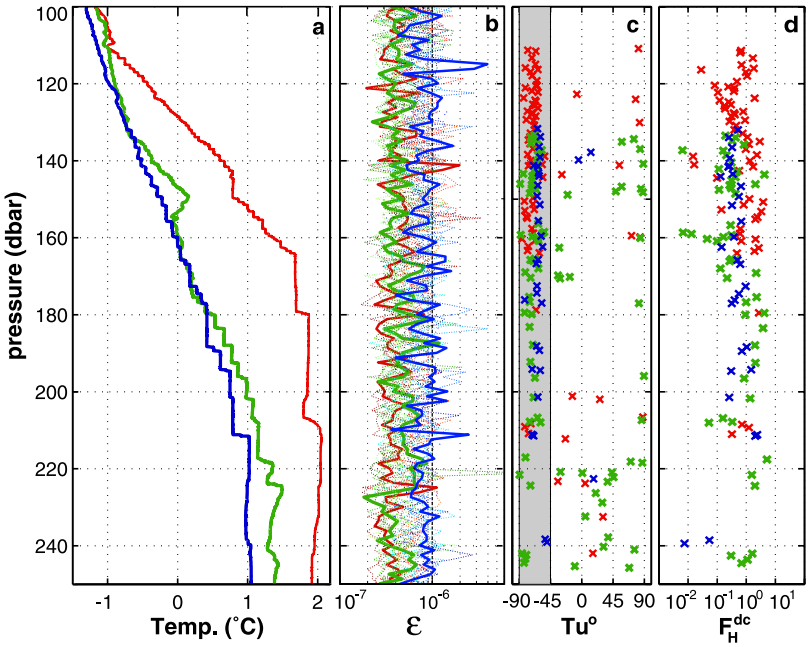

Figure 3. Microstructure observations for three typical stations on section W (red: station 7), R (green: station 21) and E (blue: station 38) of (a) temperature, (b) ϵ (W m^{-3}) (thick lines highlight stations 7, 21 and 38, dotted lines show remaining ϵ profiles), (c) Turner angle (Tu°) and (d) diffusive heat fluxes F_H^{dc} (W m^{-2}) across the steps that fall within the diffusive convection regime ($-90 < \mathrm{Tu}^\circ < -45$ indicted by gray shading in Figure 3c). Note that ϵ and the heat fluxes are plotted on logarithmic scales.

propagating eastwards around the Arctic boundary [*Dmitrenko et al.*, 2008]. However, by the 2007 field season, this anomaly had extended over all of the NABOS/ASBO station locations (I. Dmitrenko, personal communication, 2008). *Dmitrenko et al.* [2008] also showed that there is an eastwards cooling of the AW core in the long-term (1894–1990) mean boundary current that is also consistent with the 2007 observations. Therefore, we believe it is unlikely that upstream interannual variability is the primary reason of the spatial variation observed in 2007.

[14] Local moored observations indicate that the boundary and recirculating currents are predominantly aligned with the bathymetry [*Woodgate et al.*, 2001; *Dmitrenko et al.*, 2008]. Given the bifurcation of the boundary current at LR, it is unlikely that section R resolves all of the current passing through section W. This flow divergence would correspond to a horizontal heat flux divergence that could cool the AW core. However, section R resolves the portion of the boundary current passing through W that crosses LR in water depths shallower than the 2500-m isobath. The heat content difference (-2.7×10^8 J m^{-2}) between the southernmost (coolest) W station and the northernmost (warmest) R station can not be reconciled by the double diffusive heat fluxes alone. Further along the continental slope, the some of the coldest section E temperatures are observed at the northernmost stations (Figures 2a and 2d), perhaps indicative of MB recirculating water that has joined the boundary current.

[15] The observed cooling and freshening points to a shelf-sea source of cold fresh water being mixed into the boundary current. The densest central Laptev Sea shelf water found in winter is insufficiently dense to penetrate below the halocline [*Schauer et al.*, 1997], where the dramatic cooling is observed (Figure 2a). Dense cold fresh water formed during winter brine rejection in several localised areas in the Barents, Kara and Laptev seas [*Ivanov and Golovin*, 2007], such as nearby Severnaya Zemlya lee polynya (T ~ -0.9°C, S $\sim$ 34.7 at 200-m depths) [*Rudels et al.*, 1999], can ventilate the Arctic below the halocline. A simple dilution calculation suggests that the W-section water and Severnaya Zemlya shelf bottom water must mix in a 6:4 ratio to cool the W-thermohaline staircase down to section R temperatures. However, the polynya water is too salty to explain the observed freshening, suggesting that other fresher shelf waters are likely to be involved in the boundary current transformation.

6. Conclusions

[16] The upper-ocean microstructure and hydrographic observations on the Arctic East Siberian continental slope region in summer 2007 reveal the cooling and freshening of the boundary current as it approached and crossed the LR. In this weakly turbulent environment ($\epsilon < 10^{-6}$ W m^{-3}), molecular diffusion controls vertical mixing. However, the doubly-diffusive convection heat fluxes ($F_H^{dc} \sim 1$ W m^{-2}) failed to account for the significantly larger alongstream differences in upper-ocean heat-content observed. This implicates flow patterns of the boundary and recirculation currents, and lateral mixing with dense water convecting off the continental shelves and other fresher shelf waters in causing the observed evolution of the Arctic boundary current water properties.

[17] **Acknowledgments.** This study was supported by the UK Natural Environment Research Council ASBO IPY Consortium grant. The authors thank their partners at IARC, Fairbanks, and the captain and crew of the Viktor Buynitsky. We acknowledge Ben Powell for his essential technical support, and are grateful to our reviewers for their constructive comments.

References

Abrahamsen, E. P., et al. (2008), Tracer-derived freshwater composition of the Siberian Continental Shelf following the extreme Arctic summer of 2007, manuscript in preparation.

Carmack, E. (2000), The Arctic Ocean's freshwater budget: Sources, storage and export, in *The Freshwater Budget of the Arctic Ocean*, *NATO Sci. Ser., 2*, vol. 70, edited by E. L. Lewis, pp. 91–126, Kluwer, Amsterdam.

Dmitrenko, I. A., I. V. Polyakov, S. A. Kirillov, L. A. Timokhov, I. E. Frolov, V. T. Sokolov, H. L. Simmons, V. V. Ivanov, and D. Walsh (2008), Toward a warmer Arctic Ocean: Spreading of the early 21st century Atlantic Water warm anomaly along the Eurasian Basin margins, *J. Geophys. Res.*, *113*, C05023, doi:10.1029/2007JC004158.

Environmental Working Group (1997–1998), *Joint U. S.-Russian Atlas of the Arctic Ocean* [CD-ROM], Natl. Snow and Ice Data Cent., Boulder, Colo.

Gargett, A. E. (1988), The scaling of turbulence in the presence of stable stratification, *J. Geophys. Res.*, *93*, 5021–5036.

Inoue, R., H. Yamazaki, F. Wolk, T. Kono, and J. Yoshida (2007), An estimation of buoyancy flux for a mixture of turbulence and double diffusion, *J. Phys. Oceanogr.*, *37*, 611–623.

Ivanov, V. V., and P. N. Golovin (2007), Observations and modeling of dense water cascading from the northwestern Laptev Sea shelf, *J. Geophys. Res.*, *112*, C09003, doi:10.1029/2006JC003882.

Kelley, D. E. (1990), Fluxes through diffusive staircases: A new formulation, *J. Geophys. Res.*, *95*, 3365–3371.

May, B. D., and D. E. Kelley (2001), Growth and steady state stages of the thermohaline intrustion in the Arctic Ocean, *J. Geophys. Res.*, *106*, 16,783–16,794.

Meincke, J., B. Rudels, and H. J. Friedrich (1997), The Arctic Ocean–Nordic Seas thermohaline system, *ICES J. Mar. Sci.*, *54*, 283–299.

Perovich, D. K., J. A. Richter-Menge, K. F. Jones, and B. Light (2008), Sunlight, water, and ice: Extreme Arctic sea ice melt during the summer of 2007, *Geophys. Res. Lett.*, *35*, L11501, doi:10.1029/2008GL034007.

Rainville, L., and P. Winsor (2008), Mixing across the Arctic Ocean: Microstructure observations during the Beringia 2005 Expedition, *Geophys. Res. Lett.*, *35*, L08606, doi:10.1029/2008GL033532.

Rippeth, T. P., J. H. Simpson, E. Williams, and M. E. Inall (2003), Measurement of the rates of production and dissipation of turbulent kinetic energy in an energetic tidal flow: Red Wharf Bay revisited, *J. Phys. Oceanogr.*, *33*, 1889–1901.

Ruddick, B. R. (1983), A practical indicator of the stability of the water column, *Deep Sea Res., Part A*, *30*, 1105–1107.

Rudels, B., E. P. Jones, L. G. Anderson, and G. Kattner (1994), On the intermediate depth waters of the Arctic Ocean, in *The Polar Oceans and Their Role in Shaping the Global Environment*, *Geophysics Monogr. Ser.*, vol. 85, edited by O. Johannessen, R. Muench, and J. Overland, pp. 33–46, AGU, Washington., D. C.

Rudels, B., G. Björk, R. Muench, and U. Schauer (1999), Double-diffusive layering in the Eurasian Basin of the Arctic Ocean, *J. Mar. Syst.*, *21*, 3–27.

Schauer, U., R. D. Muench, B. Rudels, and L. Timokhov (1997), Impact of eastern Arctic shelf waters on the Nansen Basin intermediate layers, *J. Geophys. Res.*, *102*, 3371–3382.

Schauer, U., H. Loeng, B. Rudels, V. K. Ozhigin, and W. Dieck (2002), Atlantic Water flow through the Barents and Kara seas, *Deep Sea Res., Part I*, *49*(12), 2281–2298.

Sundfjord, A., I. Fer, Y. Kasajima, and H. Svendsen (2007), Observations of turbulent mixing and hydrography in the marginal ice zone of the Barents Sea, *J. Geophys. Res.*, *112*, C05008, doi:10.1029/2006JC003524.

Woodgate, R. A., K. Aagaard, R. Muench, J. Gunn, G. Björk, B. Rudels, A. Roach, and U. Schauer (2001), The Arctic Ocean Boundary Current along the Eurasian slope and the adjacent Lomonosov Ridge: Water mass properties, transport and transformations from moored instruments, *Deep Sea Res., Part I*, *48*, 1757–1792.

E. P. Abrahamsen, British Antarctic Survey, Natural Environment Research Council, Cambridge CB3 0ET, UK.

S. Bacon and S. Torres-Valdes, National Oceanography Centre, Southampton SO14 3ZH, UK.

V. Ivanov and I. Polyakov, International Arctic Research Center, University of Alaska Fairbanks, Fairbanks, AK 99775-7220, USA.

S. Kirillov, Arctic and Antarctic Research Institute, St. Petersburg 199397, Russia.

S. W. Laxon, Centre for Polar Observation and Modelling, University College London, London WC1E 6BT, UK.

Y. D. Lenn, T. P. Rippeth, J. H. Simpson, and P. J. Wiles, School of Ocean Sciences, Bangor University, Menai Bridge, Bangor, LL59 5AB, UK. (y.lenn@bangor.ac.uk)